



An optimized formula for the two-point resistance of a cobweb resistance network and its potential application*

Yu GUAN¹, Xiaoyu JIANG^{†‡1}, Yanpeng ZHENG^{†‡2}, Zhaolin JIANG³

¹School of Information Science and Engineering, Linyi University, Linyi 276000, China

²School of Automation and Electrical Engineering, Linyi University, Linyi 276000, China

³School of Mathematics and Statistics, Linyi University, Linyi 276000, China

[†]E-mail: jxy19890422@sina.com; zhengyanpeng0702@sina.com

Received July 21, 2024; Revision accepted Oct. 10, 2024; Crosschecked

Abstract: In recent years, the exploration and application of resistance networks have expanded significantly, and solving the equivalent resistance between two points of a resistance network has been an important topic. In this paper, we focus on optimizing the formula for calculating the two-point resistance of an $m \times n$ cobweb resistance network with $2r$ boundary conditions. To improve the computational efficiency of the equivalent resistance between two points, the formula is optimized by using the optimal approximation property of Chebyshev polynomials in combination with hyperbolic functions, and the derivation process is simplified. We discussed the equivalent resistance formulas in several special cases and compared the computational efficiency of the equivalent resistance formulas before and after optimization. Finally, we made an innovative attempt of path planning through potential formulas and proposed a heuristic algorithm based on cobweb potential function for robot path planning in a cobweb environment with obstacles.

Key words: Resistance network; Equivalent resistance; Potential function; Chebyshev polynomials; Path planning
<https://doi.org/10.1631/FITEE.2400613>

CLC number:

1 Introduction

With the continuous progress of modern science, many fields are facing increasingly complex problems. Further exploration by the researchers found that building a resistance network model (Kirchhoff, 1847; Pennetta et al., 2004; Ferri and Antonini, 2007; Owaidat et al., 2012; Rhazaoui et al., 2013; Liu et al., 2016; Hadad et al., 2018; Zhang et al., 2021; Xu et al., 2021) can help to solve some of these problems. Since Kirchhoff's law (Kirchhoff, 1847) laid the foundation for the research of resistance networks, after more than 170 years of in-depth exploration, the research of resistance networks has made

remarkable progress and researchers have proposed some new methods.

In the early days, the research of resistance networks focused on infinite network structures, and Cserti et al. (Cserti et al., 2002) opened a completely new path for the exploration of infinite resistance networks by introducing the Green's function technique. Subsequently, the equivalent resistance values between any two points in various infinite lattice resistance structures were accurately computed using this method (Cserti et al., 2011), and the method was extended to deal with perturbed lattice problems containing one missing bond (Giordano, 2007). Since then, Green's function techniques have been gradually applied to the research of infinite networks, and some new theoretical results have been obtained (Giordano, 2007; Hijjawi et al., 2008; Guttmann, 2010; Kook, 2011; Asad et al., 2013; Asad, 2013a,b).

[‡] Corresponding authors

* Project supported by the National Natural Science Foundation of China (No. 12101284), the Natural Science Foundation of Shandong Province (No. ZR2022MA092) and the Department of Education of Shandong Province (No. 2023KJ214)

© Zhejiang University Press 2024

However, an infinite network is an ideal structure that does not take boundary conditions into account, and Green's function techniques are not applicable to finite networks. The initial exploration of finite networks can be traced back to the research of Klein and Randić (Klein and Randić, 1993), which was subsequently explored in more depth by Klein et al. (Klein, 2010; Yang and Klein, 2013). Meanwhile, Wu (Wu, 2004) proposed the Laplace matrix method to calculate the resistance between arbitrary nodes in a finite resistance lattice, which has been widely used in subsequent studies (Tzeng and Wu, 2006; Izmailian et al., 2014; Izmailian and Kenna, 2014; Essam et al., 2014; Izmailian and Kenna, 2015; Essam et al., 2015). Specifically, Essam and Wu (Essam and Wu, 2009) used the method to successfully find the exact value of the site-to-site resistance and its asymptotic expansion under free boundary conditions, while Izmailian and Huang (Izmailian and Huang, 2010) further extended it to compute the resistance values under many different boundary conditions. However, the resistance between arbitrary nodes with complex boundary conditions cannot be solved using the Laplace method.

To overcome the shortcomings of previous theories, in 2013, Tan (Tan et al., 2013) creatively introduced the recursive transformation (*RT*) method, which opened up a new path for the study of resistance networks. Compared with the traditional Laplacian method that relies on two direction matrices, this method only relies on one direction matrix, which simplifies the solving process and makes the solution more convenient for example, solving the resistance between two points in a cobweb with complex boundary conditions (Tan and Fang, 2015), which is equivalent resistance. Subsequently, Tan utilized the *RT* method to explore the electrical characteristics of resistance networks and made significant contributions to the development of the field (Tan, 2017; Tan and Tan, 2020a,b,c; Tan, 2022, 2023,?; Luo and Tan, 2023; Chen et al., 2024). The core of the *RT* method is to construct a recursive matrix equation containing tridiagonal matrix. Nowadays, tridiagonal matrices have been widely studied (Wei et al., 2019a,b; Jiang et al., 2019; Wei et al., 2020; Fu et al., 2020a,b; Meng et al., 2021; Wei et al., 2022; Meng et al., 2022; Meng et al.; Wang et al., 2023). In addition, neural networks (Wang et al.,

2017; Shi et al., 2022; Jin et al., 2022a; Sun et al., 2022; Hu and Zheng, 2023; Jin et al., 2022b; Wu and Zhang, 2024) also have similarities to resistance networks.

It is worth mentioning that Tan ingeniously established a mathematical model of a cobweb resistance network with $2r$ boundary resistance (Tan and Fang, 2015), which theoretically gives an incomparable accurate formula for the equivalent resistance between any two points. However, as the scale of the cobweb resistance network increases, the original resistance formula gradually reveals deficiencies in terms of computational performance and scalability. To compensate for these deficiencies, in this paper, Chebyshev polynomials of the second kind (Udrea, 1996; Mason and Handscomb, 2002) combined with hyperbolic functions are used to re-express the exact formula for the equivalent resistance between any two points, which significantly improves the computational efficiency. In recent years, some progress has been made in large-scale potential calculation (Zhou et al., 2022, 2023; Jiang et al., 2023; Zhao et al., 2023; Jiang et al., 2024), which also provides ideas for this research.

Different from the existing research results, this paper focuses on a new resistance network model, the cobweb, which is re-represented by using Chebyshev polynomials of the second kind combined with hyperbolic functions on the basis of the original equivalent resistance formula between two points, giving the rederived equivalent resistance formula and the related proofs. By optimizing the original resistance formula, not only the derivation process is simplified but also the optimal approximation property of Chebyshev polynomials is skillfully incorporated, which significantly improves the computational efficiency and practicality of the optimized formula. Considering the influence of parameters on the equivalent resistance formula, the equivalent resistance formulas in several special cases are discussed in this paper and demonstrated in three-dimensional graphs. Comparative experiments on the equivalent resistance formulas before and after optimization reveal that the optimization greatly reduces the time cost. The equivalent resistance formula proposed in this paper is very suitable for application to large-scale complex networks due to its high computational efficiency.

In addition, path planning methods have been

extensively studied and applied in various fields, including collaborative mobile robots using discrete event models (Mahulea et al., 2020), improved artificial potential fields for multi-UAV path optimization and control (Pan et al., 2022), hybrid methods combining water flow potential fields with beetle antennae search for mobile robot path planning (Yu et al., 2023), automatic ship collision avoidance (Zhu et al., 2023), and 3D potential field models for local path planning of autonomous vehicles (Ji et al., 2023). In recent years, with in-depth research on path planning problems with specific shapes by researchers, a series of important achievements have emerged. Aybars (Uğur, 2008) and Xue et al. (Xue et al., 2021) have achieved breakthroughs in path planning research on cuboids and cylinders, respectively, while Gisala Kulatunga (Kulathunga, 2022) and Mazaheri et al. (Mazaheri et al., 2024) have made a significant progress in path planning in 3D environments. These studies fully demonstrate the examples of path planning in special environments. In this context, based on the potential function of the cobweb resistance network, a path planning algorithm for robot in a cobweb environment is proposed. The algorithm makes a good use of the characteristics of the resistance network, and plans the motion path of robot in the cobweb environment by precise potential function, and realizes efficient and accurate path planning.

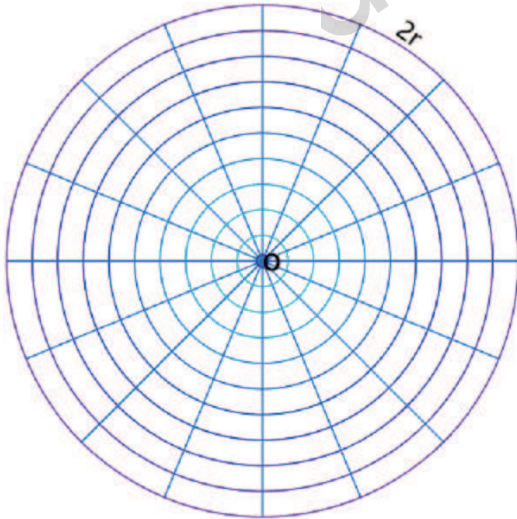


Fig. 1 A 10×16 cobweb with a $2r$ boundary, containing 10×16 nodes and a zero potential point O .

In 2015, Tan (Tan and Fang, 2015) proposed an $m \times n$ cobweb resistor network with $2r$ boundaries,

which has n radial lines and m polygons (or circle). Bonds in the radial and arc directions represent resistors r_0 and r , respectively, except for a $2r$ boundary, and let O be the origin of the coordinate system as shown in Fig. 1. Point $O(0,0) = 0$ is defined as the origin of the resistance network. Assume that the input and output points of current J are represented by d_1 and d_2 , respectively. The equivalent resistance between any two points $d_1(0, y_1)$ and $d_2(x, y_2)$ is as follows

$$R_{m \times n}(\{0, y_1\}, \{x, y_2\}) = \frac{2r}{m} \sum_{i=1}^m \frac{F_n^{(i)}(S_{1,i}^2 + S_{1,i}^2) - 2(F_x^{(i)} + F_{n-x}^{(i)})S_{1,i}S_{2,i}}{\lambda_i^n + \bar{\lambda}_i^n - 2}, \quad (1)$$

where

$$F_k^{(i)} = (\lambda_i^k - \bar{\lambda}_i^k) / (\lambda_i - \bar{\lambda}_i), \quad (2)$$

$$h = r/r_0, \quad \lambda_k \bar{\lambda}_k = 1, \quad (3)$$

$$S_{k,i} = \sin(y_k \theta_i), \quad \theta_i = (2i-1)\pi/(2m), \quad (4)$$

$$i = 1, 2, \dots, m,$$

and

$$\lambda_i = 1 + h - h \cos \theta_i + \sqrt{(1 + h - h \cos \theta_i)^2 - 1}, \quad (5)$$

$$\bar{\lambda}_i = 1 + h - h \cos \theta_i - \sqrt{(1 + h - h \cos \theta_i)^2 - 1}. \quad (6)$$

2 Optimized formula of resistance represented by Chebyshev polynomials

In this section, the resistance formula (1) for representing the cobweb resistance network is introduced. The equivalent resistance expression represented by Chebyshev polynomials of the second kind can improve the calculation efficiency.

Let us consider a scenario where a current J flows in at $d_1(0, y_1)$ with $0 \leq y_1 \leq m$ and flows out at $d_2(x, y_2)$ with $0 \leq x \leq n$ and $0 \leq y_2 \leq m$. The new resistance formula for the resistance of the $m \times n$ cobweb resistance network with a $2r$ boundary condition can be expressed as follows:

$$R_{m \times n}(\{0, y_1\}, \{x, y_2\}) = \frac{2r}{m} \sum_{j=1}^m \frac{U_{n-1}^{(j)}(S_{1,j}^2 + S_{2,j}^2) - 2(U_{x-1}^{(j)} + U_{n-x-1}^{(j)})S_{1,j}S_{2,j}}{U_n^{(j)} - U_{n-2}^{(j)} - 2}, \quad (7)$$

where

$$U_k^{(j)} = U_k^{(j)}(\cosh \psi_j) = \frac{\sinh(k+1)\psi_j}{\sinh(\psi_j)}, \quad (8)$$

$$\cosh \psi_j = \frac{\kappa_j}{2}, \quad \frac{\kappa_j}{2} > 1, \quad \psi_j > 0,$$

$$\kappa_j = 2 + 2\frac{r}{r_0} - 2\frac{r}{r_0} \cos \frac{(2j-1)\pi}{2m}, \quad (9)$$

$$S_{k,j} = \sin\left(\frac{y_k(2j-1)\pi}{2m}\right), \quad k = 1, 2. \quad (10)$$

3 Optimization process of original function

In this section, to improve the actual performance, we introduce Horadam sequence represented by Chebyshev polynomials of the second kind (Udrea, 1996; Mason and Handscomb, 2002).

Horadam sequence is defined by the following conditions (Udrea, 1996):

$$W_k = dW_{k-1} - qW_{k-2}, \quad W_0 = A, \quad W_1 = B, \quad (11)$$

where $k \in \mathbf{N}$, $k \geq 2$, $A, B, d, q \in \mathbf{C}$, and \mathbf{N} are the sets of all natural numbers and \mathbf{C} is the set of all complex numbers.

We know that Horadam sequence represented by Chebyshev polynomials of the second kind (Mason and Handscomb, 2002) is as follows:

$$W_k = (\sqrt{q})^k \left(\frac{B}{\sqrt{q}} U_{k-1} \left(\frac{d}{2\sqrt{q}} \right) - A U_{k-2} \left(\frac{d}{2\sqrt{q}} \right) \right), \quad (12)$$

where

$$U_k = U_k(\cos \psi) = \frac{\sin(k+1)\psi}{\sin \psi}, \quad (13)$$

$$\cos \psi = \frac{d}{2\sqrt{q}}, \quad \psi \in \mathbf{C},$$

is Chebyshev polynomials of the second kind.

If $\frac{d}{2\sqrt{q}} > 1$, Chebyshev polynomials of the second kind are re-described by hyperbolic functions, then Eq. (13) should be expressed as follows:

$$U_k = U_k(\cosh \psi) = \frac{\sinh(k+1)\psi}{\sinh \psi}, \quad (14)$$

$$\cosh \psi = \frac{d}{2\sqrt{q}}, \quad \psi \in \mathbf{R},$$

where \mathbf{R} is the set of real number.

First, the derivation of Eq. (2) represented by Chebyshev polynomials of the second kind is given.

Remark 1: It can be obtained from Eq. (5) that $\lambda_j + \bar{\lambda}_j = \kappa_j$ and $\lambda_j \bar{\lambda}_j = 1$. By adding these conditions with Eq. (11), we obtained get the following special Horadam sequence

$$F_k^{(j)} = \kappa_j F_{k-1}^{(j)} - F_{k-2}^{(j)}, \quad F_0^{(j)} = 0, \quad F_1^{(j)} = 1, \quad (15)$$

where $d = \kappa_j > 2$, $q = 1$, $F_k^{(j)}$, and κ_j are given by Eqs (2) and (9), respectively. By using Eqs (2), (11), (12), and (14), the expression for $F_k^{(j)}$ can be obtained as follows:

$$F_k^{(j)} = \frac{\lambda_j^k - \bar{\lambda}_j^k}{\lambda_j - \bar{\lambda}_j} = U_{k-1}^{(j)}\left(\frac{\kappa_j}{2}\right). \quad (16)$$

Second, we will give the derivation of $\lambda_j^n + \bar{\lambda}_j^n$ expressed by Chebyshev polynomials of the second kind.

Remark 2: Let

$$B_n^{(j)} = \lambda_j^{(n)} + \bar{\lambda}_j^{(n)}, \quad (17)$$

where $B_0^{(j)} = 2$, $B_1^{(j)} = \kappa_j$.

Then, the recursive relation of $B_n^{(j)}$ is expressed as follows:

$$B_n^{(j)} = \kappa_j B_{n-1}^{(j)} - B_{n-2}^{(j)}, \quad B_0^{(j)} = 2, \quad B_1^{(j)} = \kappa_j, \quad (18)$$

where $d = \kappa_j$, $q = 1$, κ_j , and $B_n^{(j)}$ are expressed in Eqs (9) and (17), respectively.

By using Eqs (12) and (14), $B_n^{(j)}$ is represented as follows:

$$B_n^{(j)} = \lambda_j^{(n)} + \bar{\lambda}_j^{(n)} = \kappa_j U_{n-1}\left(\frac{\kappa_j}{2}\right) - 2U_{n-2}\left(\frac{\kappa_j}{2}\right)$$

$$= U_n\left(\frac{\kappa_j}{2}\right) - U_{n-2}\left(\frac{\kappa_j}{2}\right). \quad (19)$$

Using Eqs (14), (16), and (19), the equivalent resistance formula (7) is obtained.

4 Several interesting classes of the resistance network

This section is based on the obtained equivalent resistance formula (7) for a cobweb resistance network with multiple variables. Analyze the influence of different variables on the equivalent resistance expression, assign the corresponding variables according to the conditions, and draw a 3D view for visual display.

Special 1. When the current J flows from input point $d_1(0, y_1)$ to output point $d_2(x, y_2)$, where $y_1 = y_2$ and $S_{1,j} = S_{2,j}$, the formula for the equivalent resistance between two points is as follows:

$$R_{m \times n}(\{0, y_2\}, \{x, y_2\}) = \frac{4r}{m} \sum_{j=1}^m \left(\frac{U_{n-1}^{(j)} - (U_{x-1}^{(j)} + U_{n-x-1}^{(j)})}{U_n^{(j)} - U_{n-2}^{(j)} - 2} \right) S_{k,j}^2, \quad (20)$$

where

$$U_k^{(j)} = U_k^{(j)} (\cosh \psi_j) = \frac{\sinh(k+1)\psi_j}{\sinh(\psi_j)}, \quad (21)$$

$$\cosh \psi_j = \frac{\kappa_j}{2}, \quad \frac{\kappa_j}{2} > 1, \quad \psi_j > 0.$$

$$\kappa_j = 2 + 2\frac{r}{r_0} - 2\frac{r}{r_0} \cos \frac{(2j-1)\pi}{2m}, \quad (22)$$

$$S_{k,j} = \sin\left(\frac{y_k(2j-1)\pi}{2m}\right), \quad k = 1, 2, \quad (23)$$

Let $m = n = 60$ and $r_0 = r = 1$ in Eq. (20), respectively. We can obtain a special resistance formula for the cobweb resistance network as follows:

$$R_{60 \times 60}(\{0, y_2\}, \{x, y_2\}) = \frac{1}{15} \sum_{j=1}^{60} \left(\frac{U_{59}^{(j)} - (U_{x-1}^{(j)} + U_{59-x-1}^{(j)})}{U_{60}^{(j)} - U_{58}^{(j)} - 2} \right) S_{2,j}^2, \quad (24)$$

where

$$U_k^{(j)} = U_k^{(j)} (\cosh \psi_j) = \frac{\sinh(k+1)\psi_j}{\sinh(\psi_j)}, \quad (25)$$

$$\cosh \psi_j = \frac{\kappa_j}{2},$$

$$\kappa_j = 4 - 2 \cos \frac{(2j-1)\pi}{120}, \quad (26)$$

$$S_{2,j} = \sin\left(\frac{y_2(2j-1)\pi}{120}\right). \quad (27)$$

The 3D distribution of the equivalent resistance is shown in Fig. 2.

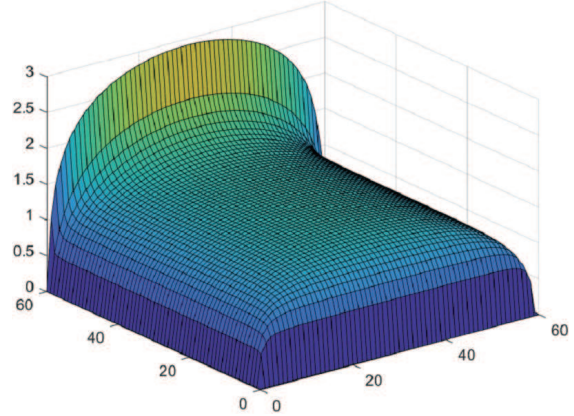


Fig. 2 The equivalent resistance view of $R_{60 \times 60}(d_1, d_2)$ with a cobweb resistance network is shown in Eq. (24).

Special 2. If the current J flows in point $d_1(0, 0) = O(0, 0)$ and out of $d_2(x, y_2)$, then the formula for the equivalent resistance between two points is as follows:

$$R_{m \times n}\{(0, 0), (x, y_2)\} = \frac{2r}{m} \sum_{j=1}^m \left(\frac{U_{n-1}^{(j)} S_{2,j}^2}{U_n^{(j)} - U_{n-2}^{(j)} - 2} \right), \quad (28)$$

where $U_k^{(j)}$ is defined in Eq. (21), κ_j is defined in Eq. (22), and $S_{k,j}$ is defined in Eq. (23).

Let $m = n = 60$ and $r_0 = r = 1$ in Eq. (28), respectively. We can obtain a special resistance formula for the cobweb resistance network as follows:

$$R_{60 \times 60}\{(0, 0), (x, y_2)\} = \frac{1}{30} \sum_{j=1}^{60} \left(\frac{U_{59}^{(j)} S_{2,j}^2}{U_{60}^{(j)} - U_{58}^{(j)} - 2} \right), \quad (29)$$

where

$$U_k^{(j)} = U_k^{(j)} (\cosh \psi_j) = \frac{\sinh(k+1)\psi_j}{\sinh(\psi_j)}, \quad (30)$$

$$\cosh \psi_j = \frac{\kappa_j}{2},$$

$$\kappa_j = 4 - 2 \cos \frac{(2j-1)\pi}{120}, \quad (31)$$

$$S_{2,j} = \sin\left(\frac{y_2(2j-1)\pi}{120}\right). \quad (32)$$

The 3D distribution of the equivalent resistance is shown in Fig. 3.

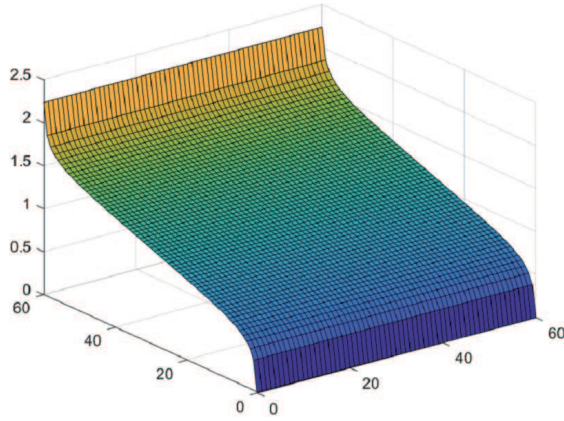


Fig. 3 The equivalent resistance view of $R_{60 \times 60}(d_1, d_2)$ with a cobweb resistance network is shown in Eq. (29).

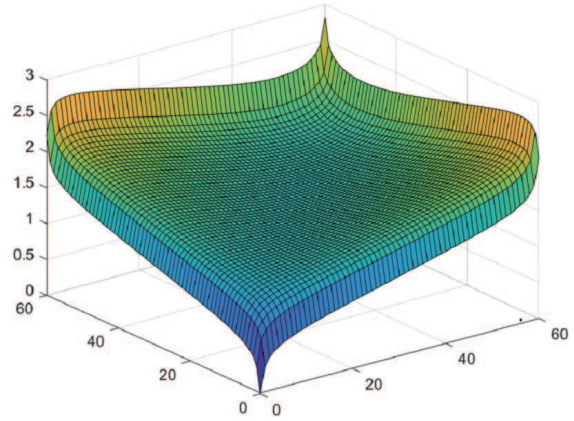


Fig. 4 The equivalent resistance view of $R_{60 \times 60}(d_1, d_2)$ with a cobweb resistance network is shown in Eq. (34).

Special 3. If the current J flows in point $d_1(0, y_1)$ and out of $d_2(20, y_2)$, then the formula for the equivalent resistance between two points is as follows:

$$R_{m \times n}\{(0, y_1), (20, y_2)\} = \frac{2r}{m} \sum_{j=1}^m \left(\frac{U_{n-1}^{(j)}(S_{1,j}^2 + S_{2,j}^2) - 2(U_{x-1}^{(j)} + U_{n-x-1}^{(j)})S_{1,j}S_{2,j}}{U_n^{(j)} - U_{n-2}^{(j)} - 2} \right), \quad (33)$$

where $U_k^{(j)}$ is defined in Eq. (21), κ_j is defined in Eq. (22), and $S_{k,j}$ is defined in Eq. (23).

Let $m = n = 60$ and $r_0 = r = 1$ in Eq. (33), respectively. We can obtain a special resistance formula for the cobweb resistance network as follows:

$$R_{60 \times 60}\{(0, y_1), (20, y_2)\} = \frac{1}{30} \sum_{j=1}^{60} \left(\frac{U_{59}^{(j)}(S_{1,j}^2 + S_{2,j}^2) - 2(U_{19}^{(j)} + U_{39}^{(j)})S_{1,j}S_{2,j}}{U_{60}^{(j)} - U_{58}^{(j)} - 2} \right), \quad (34)$$

where

$$U_k^{(j)} = U_k^{(j)}(\cosh \psi_j) = \frac{\sinh(k+1)\psi_j}{\sinh(\psi_j)}, \quad (35)$$

$$\cosh \psi_j = \frac{\kappa_j}{2},$$

$$\kappa_j = 4 - 2 \cos \frac{(2j-1)\pi}{120}, \quad (36)$$

$$S_{1,j} = \sin\left(\frac{y_1(2j-1)\pi}{120}\right), \quad (37)$$

$$S_{2,j} = \sin\left(\frac{y_2(2j-1)\pi}{120}\right).$$

The 3D distribution of the equivalent resistance is shown in Fig. 4.

Special 4. When the current J flows from input point $d_1(0, y_1)$ to output point $d_2(x, y_2)$, where $y_1 = x$, the formula for the equivalent resistance between two points is as follows:

$$R_{m \times n}\{(0, x), (x, y_2)\} = \frac{2r}{m} \sum_{j=1}^m \left(\frac{U_{n-1}^{(j)}(S_{1,j}^2 + S_{2,j}^2) - 2(U_{x-1}^{(j)} + U_{n-x-1}^{(j)})S_{1,j}S_{2,j}}{U_n^{(j)} - U_{n-2}^{(j)} - 2} \right), \quad (38)$$

where $U_k^{(j)}$ is defined in Eq. (21), κ_j is defined in Eq. (22), and $S_{k,j}$ is defined in Eq. (23).

Let $m = n = 60$ and $r_0 = r = 1$ in Eq. (38), respectively. We can obtain a special resistance formula for the cobweb resistance network as follows:

$$R_{60 \times 60}\{(0, x), (x, y_2)\} = \frac{1}{30} \sum_{j=1}^{60} \left(\frac{U_{59}^{(j)}(S_{1,j}^2 + S_{2,j}^2) - 2(U_{x-1}^{(j)} + U_{59-x}^{(j)})S_{1,j}S_{2,j}}{U_{60}^{(j)} - U_{58}^{(j)} - 2} \right), \quad (39)$$

where

$$U_k^{(j)} = U_k^{(j)}(\cosh \psi_j) = \frac{\sinh(k+1)\psi_j}{\sinh(\psi_j)}, \quad (40)$$

$$\cosh \psi_j = \frac{\kappa_j}{2},$$

$$\kappa_j = 4 - 2 \cos \frac{(2j-1)\pi}{120}, \quad (41)$$

$$S_{1,j} = \sin\left(\frac{x(2j-1)\pi}{120}\right), \quad (42)$$

$$S_{2,j} = \sin\left(\frac{y_2(2j-1)\pi}{120}\right).$$

The 3D distribution of the equivalent resistance is shown in Fig. 5.

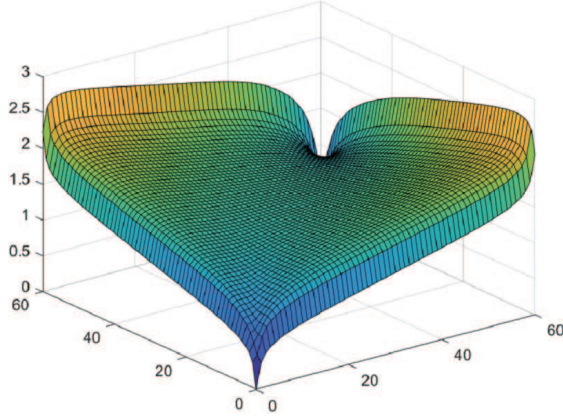


Fig. 5 The equivalent resistance view of $R_{60 \times 60}(d_1, d_2)$ with a cobweb resistance network is shown in Eq. (39).

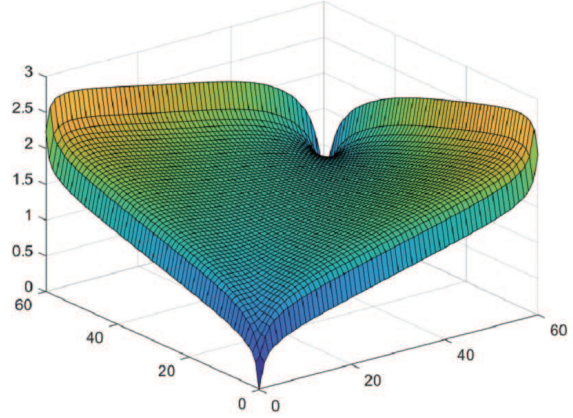


Fig. 6 The equivalent resistance view of $R_{60 \times 60}(d_1, d_2)$ with a cobweb resistance network is shown in Eq. (44).

Special 5. When the current J flows from input point $d_1(0, y_1)$ to output point $d_2(x, y_2)$, where $y_2 = x$, the formula for the equivalent resistance between two points is as follows:

$$R_{m \times n}\{(0, y_1), (x, x)\} = \frac{2r}{m} \sum_{j=1}^m \left(\frac{U_{n-1}^{(j)}(S_{1,j}^2 + S_{2,j}^2) - 2(U_{x-1}^{(j)} + U_{n-x-1}^{(j)})S_{1,j}S_{2,j}}{U_n^{(j)} - U_{n-2}^{(j)} - 2} \right), \quad (43)$$

where $U_k^{(j)}$ is defined in Eq. (21), κ_j is defined in Eq. (22), and $S_{k,j}$ is defined in Eq. (23).

Let $m = n = 60$ and $r_0 = r = 1$ in Eq. (43), respectively. We can obtain a special resistance formula for the cobweb resistance network as follows:

$$R_{60 \times 60}\{(0, y_1), (x, x)\} = \frac{1}{30} \sum_{j=1}^{60} \left(\frac{U_{59}^{(j)}(S_{1,j}^2 + S_{2,j}^2) - 2(U_{x-1}^{(j)} + U_{59-x}^{(j)})S_{1,j}S_{2,j}}{U_{60}^{(j)} - U_{58}^{(j)} - 2} \right), \quad (44)$$

where

$$U_k^{(j)} = U_k^{(j)}(\cosh \psi_j) = \frac{\sinh(k+1)\psi_j}{\sinh(\psi_j)}, \quad (45)$$

$$\cosh \psi_j = \frac{\kappa_j}{2},$$

$$\kappa_j = 4 - 2 \cos \frac{(2j-1)\pi}{120}, \quad (46)$$

$$S_{1,j} = \sin\left(\frac{y_1(2j-1)\pi}{120}\right), \quad (47)$$

$$S_{2,j} = \sin\left(\frac{x(2j-1)\pi}{120}\right).$$

The 3D distribution of the equivalent resistance is shown in Fig. 6.

Special 6. If the current J flows in point $d_1(0, y_1)$ and out of $d_2(x, 20)$, then the formula for the equivalent resistance between two points is as follows:

$$R_{m \times n}\{(0, y_1), (x, 20)\} = \frac{2r}{m} \sum_{j=1}^m \left(\frac{U_{n-1}^{(j)}(S_{1,j}^2 + S_{2,j}^2) - 2(U_{x-1}^{(j)} + U_{n-x-1}^{(j)})S_{1,j}S_{2,j}}{U_n^{(j)} - U_{n-2}^{(j)} - 2} \right), \quad (48)$$

where $U_k^{(j)}$ is defined in Eq. (21), κ_j is defined in Eq. (22), and $S_{k,j}$ is defined in Eq. (23).

Let $m = n = 60$ and $r_0 = r = 1$ in Eq. (48), respectively. We can obtain a special resistance formula for the cobweb resistance network as follows:

$$R_{60 \times 60}\{(0, y_1), (x, 20)\} = \frac{1}{30} \sum_{j=1}^{60} \left(\frac{U_{59}^{(j)}(S_{1,j}^2 + S_{2,j}^2) - 2(U_{x-1}^{(j)} + U_{59-x}^{(j)})S_{1,j}S_{2,j}}{U_{60}^{(j)} - U_{58}^{(j)} - 2} \right), \quad (49)$$

where

$$U_k^{(j)} = U_k^{(j)}(\cosh \psi_j) = \frac{\sinh(k+1)\psi_j}{\sinh(\psi_j)}, \quad (50)$$

$$\cosh \psi_j = \frac{\kappa_j}{2},$$

$$\kappa_j = 4 - 2 \cos \frac{(2j-1)\pi}{120}, \quad (51)$$

$$S_{1,j} = \sin\left(\frac{y_1(2j-1)\pi}{120}\right), \quad (52)$$

$$S_{2,j} = \sin\left(\frac{20(2j-1)\pi}{120}\right).$$

The 3D distribution of the equivalent resistance is shown in Fig. 7.

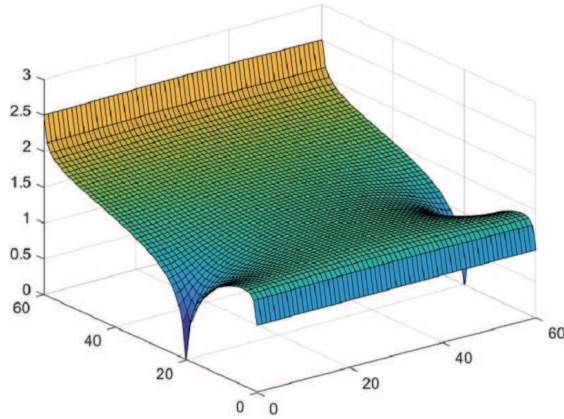


Fig. 7 The equivalent resistance view of $R_{60 \times 60}(d_1, d_2)$ with a cobweb resistance network is shown in Eq. (49).

5 Efficiency of calculation method

On the $m \times n$ scale resistance network model, $(0, y_1)$ represents the input point of current, and (x, y_2) represents the output point of the current. We compared the efficiency of resistance calculation between two methods from point $O(0, 0)$ to any point (x, y_2) . "time" refers to the total CPU time measured in seconds, with t_1 and t_2 representing the CPU time consumed for resistance calculation utilizing formulas (1) and (7), respectively.

The experiment is completed under the environmental conditions of CPU model Intel(R) Core(TM) i5-9300H CPU 2.40GHz, and MATLAB version is R2023a. " $m \times n$ " is the number of nodes in the resistance network, "-" denotes the operation time > 1200 s or beyond the memory limit of MATLAB.

Table 1 The comparison of calculation efficiency for equivalent resistance formulas (1) and (7) at $h = 1$

$m \times n$	r	r_0	h	t_1	t_2
100×100	1	1	1	0.7799	0.2353
500×500	1	1	1	92.0133	24.0147
1000×500	1	1	1	380.6860	98.6743
800×800	1	1	1	357.9222	91.4097
1000×1000	1	1	1	652.8197	180.2885
1500×1000	1	1	1	-	404.4679

Table 2 The comparison of calculation efficiency for equivalent resistance formulas (1) and (7) at $h = 10$

$m \times n$	r	r_0	h	t_1	t_2
100×100	1	0.1	10	0.7827	0.2290
500×500	1	0.1	10	78.4835	21.8411
1000×500	1	0.1	10	316.9167	88.1708
800×800	1	0.1	10	300.1308	84.5293
1000×1000	1	0.1	10	577.8685	187.3093
1500×1000	1	0.1	10	-	369.5674

Table 3 The comparison of calculation efficiency for equivalent resistance formulas (1) and (7) at $h = 0.1$

$m \times n$	r	r_0	h	t_1	t_2
100×100	0.1	1	0.1	0.7750	0.3874
500×500	0.1	1	0.1	113.9321	25.6996
1000×500	0.1	1	0.1	385.4453	101.4138
800×800	0.1	1	0.1	400.6745	103.6280
1000×1000	0.1	1	0.1	786.0421	206.0119
1500×1000	0.1	1	0.1	-	458.0859

Remark 3: By comparing the data in Tables 1, 2, and 3, we can clearly observe that the optimized equivalent resistance formula (7) exhibits a significant advantage in computational efficiency compared with the original equivalent resistance formula (1) as the network scale gradually expands under the premise that the resistance ratio remains unchanged. When the scale increases to a certain extent, the original formula is no longer suitable for numerical calculations, but the optimized formula can. In addition, we can also find that the resistivity (r/r_0) has a significant effect on the calculation of the equivalent resistance while keeping the network size consistent.

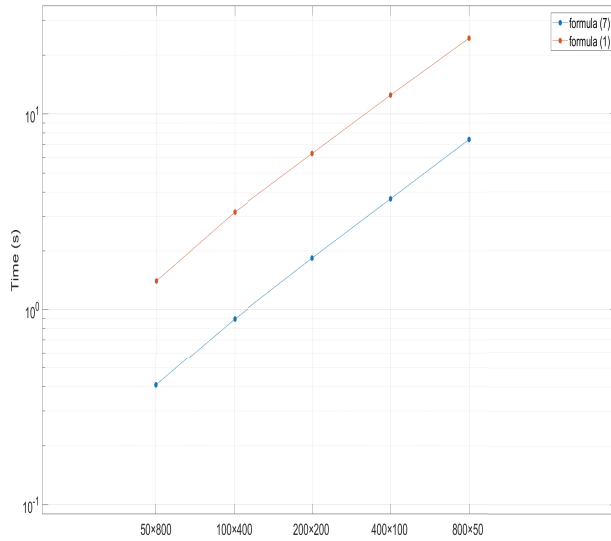


Fig. 8 Comparison of the calculation efficiency of formulas (1) and (7) when $h = 1$.

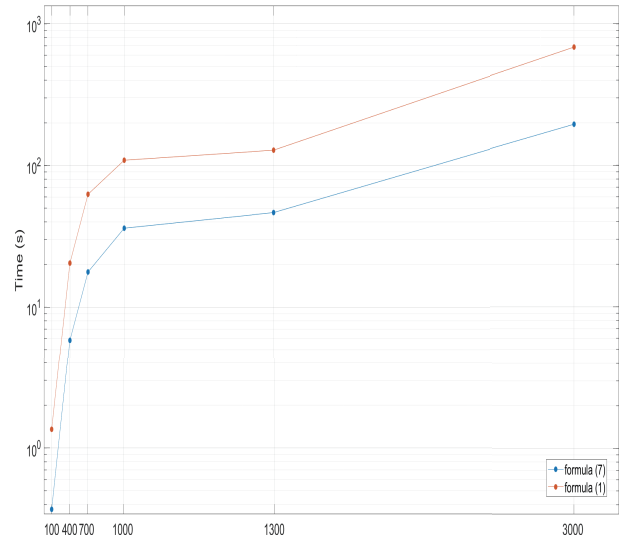


Fig. 10 Comparison of the computational efficiency between formulas (1) and (7) as m increases, with $h = 1$ and $n = 100$.

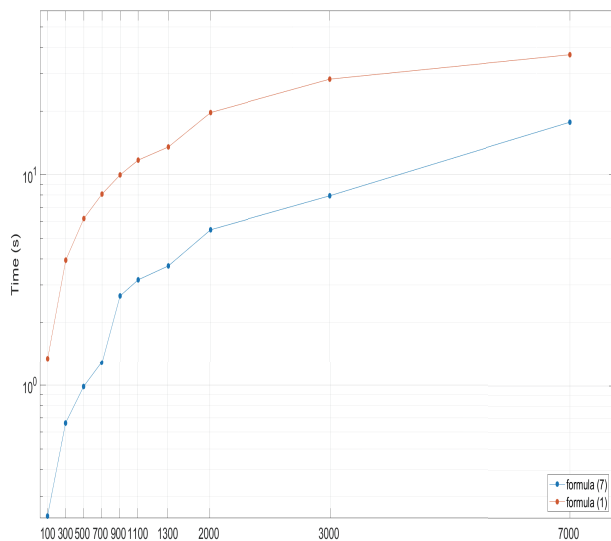


Fig. 9 Comparison of the computational efficiency between formulas (1) and (7) as n increases, with $h = 1$ and $m = 100$.

Remark 4: As can be observed from Fig. 8, when the total number of nodes (i.e., $m \times n$) in the resistance network is kept constant, the time required for computation shows an increasing trend as m increases. However, regardless of these variations, the computational efficiency of Eq. (7) is always higher than Eq. (1). In Fig. 9, where we keep m constant, the computation time increases significantly when $n > 500$. Similarly, Fig. 10 demonstrates the comparison of computational efficiency before and after optimization of the resistance formula when n is kept constant and m is gradually increased. The computation time increases significantly when $m > 1000$. In particular, the computation time of Eq. (1) increases more significantly. Combining the data in Figs 8, 9, and 10, it can be clearly seen that the optimized equivalent resistance formula (7) exhibits significant superiority when dealing with large-scale networks.

6 An application of the potential function

In 2017, Tan (Tan, 2017) first used the $RT - V$ method to study the cobweb resistance network and derived the potential function of the cobweb resistance network. In 2023, Zhao et al. (Zhao et al., 2023) optimized the potential function of the cobweb resistance network and proposed the cobweb resistance network potential function expressed by Chebyshev polynomials of the second kind. The po-

tential function of the cobweb resistance network is as follows(Zhao et al., 2023):

$$\frac{U_{m \times n}(x, y)}{J} = \frac{4r}{2m+1} \sum_{l=1}^m \frac{\mu_{x_1, x}^{(l)} S_{y_1, l} - \mu_{x_2, x}^{(l)} S_{y_2, l}}{U_n^{(l)} - U_{n-2}^{(l)} - 2} S_{y, l}, \quad (53)$$

where

$$\mu_{x_s, x}^{(l)} = U_{n-|x_s-x|-1}^{(l)} + U_{|x_s-x|-1}^{(l)}, \quad (54)$$

$$s = 1, 2,$$

$$S_{y_k, l} = \sin\left(\frac{y_k(2l-1)\pi}{2m+1}\right), \quad (55)$$

$$k = 1, 2,$$

$$\omega_l = 2 + \frac{2r}{r_0} - \frac{2r}{r_0} \cos\left(\frac{(2l-1)\pi}{2m+1}\right), \quad (56)$$

$$U_v^{(l)} = U_v^{(l)}(\cosh \phi_l) = \frac{\sinh(v+1)\phi_l}{\sinh(\phi_l)}, \quad (57)$$

$$\cosh \phi_l = \frac{\omega_l}{2}, \quad \frac{\omega_l}{2} > 1, \quad \phi_l > 0,$$

$$v = n - |x_s - x| - 1, \quad |x_s - x| - 1, \quad n - 2, \quad n,$$

$$s = 1, 2, \quad l = 1, 2, \dots, m.$$

The exact potential function of cobweb is based on the study by Zhao et al.(Zhao et al., 2023) This section carefully studies and designs a path planning strategy specifically for the cobweb environment, namely the exact potential energy formula path planning method. The method adopts a heuristic algorithm, and its core principle is to realize effective path planning through the direction of the node with the greatest potential energy decline. In the cobweb environment, the input and output points of the current correspond to the highest and lowest potential nodes respectively. The potential distribution is characterized by an irregular natural decline from the high-potential node to the low-potential node. In the case of obstacles, the nodes corresponding to the obstacle position are weighed by high potential. Ultimately, a collision free optimization path will be formed from the highest potential point to the lowest potential point direction. Next, we will provide a detailed introduction to the implementation details of the path planning algorithm.

Path planning algorithm

- Step1:** Establish a map of the robot's working environment using the grid method (determine the robot's starting point, target point, and obstacles);
- Step2:** The current input point in the cobweb resistance network is the starting point, and the current output point is the target point. Use formula (53) to calculate the potential $\frac{U(x, y)}{J}$ of each node in the cobweb resistance network;
- Step3:** Add a fixed increment to the potential of the corresponding nodes in the cobweb resistance network that correspond to the grid points where obstacles are located. The potential after adding a fixed increment is $\frac{U(x, y)}{J} + 0.3 \frac{U(x_1, y_1)}{J}$;
- Step4:** Utilize $\min\{U_{x+1, y+1}, U_{x+1, y}, U_{x+1, y-1}, U_{x, y-1}, U_{x-1, y-1}, U_{x-1, y}, U_{x-1, y+1}, U_{x, y+1}\}$ to identify the node with the minimum potential;
- Step5:** Move the robot to the corresponding grid point based on the node identified in Step 4 and update the current location;
- Step6:** If the robot's current location matches the target point, terminate the algorithm; otherwise, proceed to Step 4;
- Step7:** End of the algorithm.
-

Fig. 11 shows a simulation experiment conducted in the physical environment of a 10×16 cobweb with obstacles, where the red triangle represents the obstacles, the green ball represents the starting point, and the yellow five-pointed star represents the end point. Let $x_1 = 11, y_1 = 9, x_2 = 6, y_2 = 2, r = 1, r_0 = 1,$ and $J = 1,$ we can derive the potential discrete distribution potential diagram based on the optimized formula (53) proposed by Zhao et al.(Zhao et al., 2023) The discrete distribution of electric potential is shown in Fig. 12.

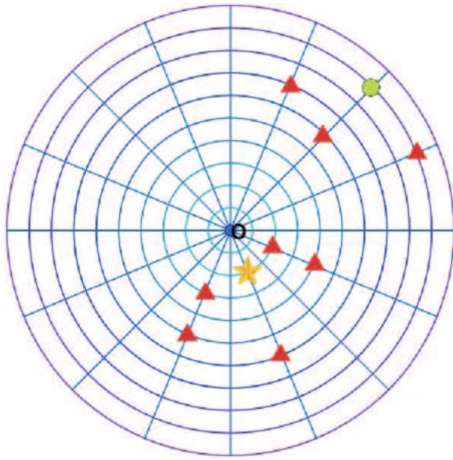


Fig. 11 A physical map of a 10×16 cobweb with obstacles.

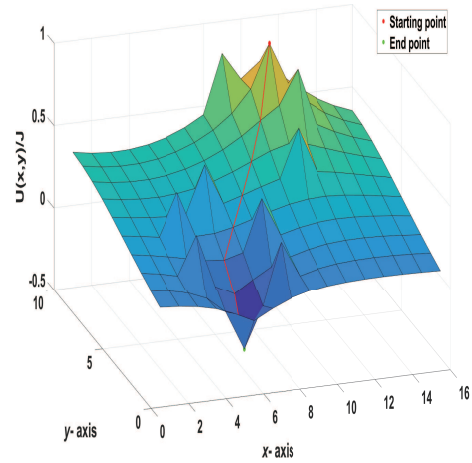


Fig. 13 Path planning in node-weighted potential distribution map.

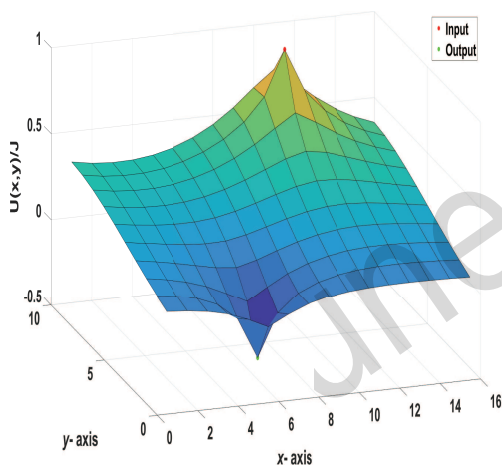


Fig. 12 Obstacle-free potential distribution diagram.

In an environment with obstacles, we weight the node potential value corresponding to the location of each obstacle. This strategy allows the robot to efficiently avoid obstacles during path planning, enabling smooth obstacle avoidance operations. This ensures that the final path is optimized to move from the high-potential node to the low-potential node. Subsequently, we demonstrated this effect through a simulation experiment, where Fig. 13 shows the path planning in the node weighted potential distribution map. Additionally, Fig. 14 corresponds to the robot path planning in a physical cobweb environment.

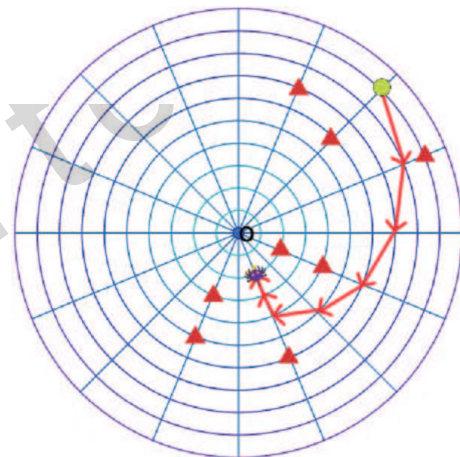


Fig. 14 Robot path planning in a physical cobweb environment.

In the robot path planning diagram in the physical cobweb environment shown in Fig. 14, the green ball represents the starting point, the yellow five-pointed star represents the end point, and the red triangle represents the obstacle. The purple spider represents the robot, and the solid line with the red arrow represents the robot's path. Through this example, we can clearly see the application effect of the cobweb resistance network in path planning.

Looking ahead, we will comprehensively utilize various strategies such as gradient descent and the establishment of subgoals to further delve into robot path planning in cobweb environments with obstacles, aiming to achieve more precise and efficient planning results.

7 Conclusions

In this paper, the equivalent resistance formula between two points of an $m \times n$ cobweb resistance network with a $2r$ boundary is improved using Chebyshev polynomials of the second kind combined with hyperbolic functions. The optimized equivalent resistance formula (7) cleverly utilizes the optimal approximation property of Chebyshev polynomials, which not only improves the computational efficiency but also simplifies the derivation process. Based on the comparison of the computational efficiency of the equivalent resistance formula before and after optimization, it is found that the computational efficiency is improved by more than three times at the same scale. This is especially obvious as the size of the resistance network increases. In addition, considering the influence of parameters on the equivalent resistance formula, this paper discusses the equivalent resistance formula for several special cases, which are presented through 3D dynamic views.

In this paper, we also attempted to perform path planning with respect to the cobweb potential function and successfully developed a heuristic algorithm to accomplish path planning by simulating potential descent. The process of finding paths in this algorithm is actually an exploration using the numerical results of the potentials to find the paths on the circuit from the input point to the output point. In an environment with obstacles, weighting the value of the node potential at the obstacle enables the robot to effectively avoid the obstacle during the path planning process and ensures that the robot can quickly approach the target point from the start point based on the potential descent trend. The effectiveness of the algorithm is also demonstrated through specific numerical simulation experiments.

Contributors

Xiaoyu, JIANG and Yanpeng, ZHENG conceived the project, performed and analyzed formulae calculations. Yu, GUAN validated the correctness of the formula calculation, and realized graph drawing. Zhaolin, JIANG proposed an improved formula for calculating equivalent resistance. All authors contributed equally to the manuscript.

Conflict of interest

All the authors declare that they have no conflict of interest.

Data availability

Data will be made available on request.

References

- Asad JH, Diab AA, Hijjawi RS, et al., 2013. Infinite face-centered-cubic network of identical resistors: Application to lattice Green's function. *Eur Phys J Plus*, 128(1):2.
<https://doi.org/10.1140/epjp/i2013-13002-8>
- Asad JH, 2013a. Exact Evaluation of the Resistance in an Infinite Face-Centered Cubic Network. *J Stat Phys*, 150(6):1177-1182.
<https://doi.org/10.1007/s10955-013-0716-x>
- Asad JH, 2013b. Infinite simple 3D cubic network of identical capacitors. *Mod Phys Lett B*, 27(15):1350112.
<https://doi.org/10.1142/S0217984913501121>
- Chen JQ, Ji WY, Tan ZZ, 2024. Electrical properties of a $2 \times n$ non-regular hammock network. *Indian J Phys*, 98(8):2851-2860.
<https://doi.org/10.1007/s12648-023-03027-w>
- Cserti J, D'Ávid G, PirÁstth A, 2002. Perturbation of infinite networks of resistors. *Am J Phys*, 70(2):153-159.
<https://doi.org/10.1119/1.1419104>
- Cserti J, SzÁlchenyi G, D'Ávid G, 2011. Uniform tiling with electrical resistors. *J Phys A: Math Theor*, 44(21):215201.
<https://doi.org/10.1088/1751-8113/44/21/215201>
- Essam JW, Tan ZZ, Wu FY, 2014. Resistance between two nodes in general position on an $m \times n$ fan network. *Phys Rev E*, 90(3):032130.
<https://doi.org/10.1103/PhysRevE.90.032130>
- Essam JW, Wu FY, 2009. The exact evaluation of the corner-to-corner resistance of an $M \times N$ resistor network: asymptotic expansion. *J Phys A: Math Theor*, 42(2):025205.
<https://doi.org/10.1088/1751-8113/42/2/025205>
- Essam JW, Izmailyan NS, Kenna R, et al., 2015. Comparison of methods to determine point-to-point resistance in nearly rectangular networks with application to a 'hammock' network. *Royal Soc Open Sci*, 2(4):140420.
<https://doi.org/10.1098/rsos.140420>
- Ferri G, Antonini G, 2007. Ladder-network-based model for interconnects and transmission lines time delay and cutoff frequency determination. *J Circuit Syst Comp*, 16(4):489-505.
<https://doi.org/10.1142/S0218126607003794>
- Fu YR, Jiang XY, Jiang ZL, et al., 2020a. Inverses and eigenpairs of tridiagonal Toeplitz matrix with opposite-bordered rows. *J Appl Anal Comput*, 10(4):1599-1613.
<https://doi.org/10.11948/20190287>
- Fu YR, Jiang XY, Jiang ZL, et al., 2020b. Properties of a class of perturbed Toeplitz periodic tridiagonal matrices. *Comput Appl Math*, 39(3):146.
<https://doi.org/10.1007/s40314-020-01171-1>

- Giordano S, 2007. Two-dimensional disordered lattice networks with substrate. *Physica A*, 375(2):726-740. <https://doi.org/10.1016/j.physa.2006.09.026>
- Guttman AJ, 2010. Lattice Green's functions in all dimensions. *J Phys A: Math Theor*, 43(30):305205. <https://doi.org/10.1088/1751-8113/43/30/305205>
- Hadad Y, Soric JC, Khanikaev AB, et al., 2018. Self-induced topological protection in nonlinear circuit arrays. *Nat Electron*, 1(3):178-182. <https://doi.org/10.1038/s41928-018-0042-z>
- Hijjawi RS, Asad JH, Sakaji AJ, et al., 2008. Infinite simple 3D cubic lattice of identical resistors (two missing bonds). *Eur Phys J Appl Phys*, 41(2):111-114. <https://doi.org/10.1051/epjap:2008015>
- Hu Q, Zheng B, 2023. An efficient takagi-sugeno fuzzy zeroing neural network for solving time-varying sylvester equation. *IEEE Trans Fuzzy Syst*, 31(7):2401-2411. <https://doi.org/10.1109/TFUZZ.2022.3225630>
- Izmailian NS, Huang MC, 2010. Asymptotic expansion for the resistance between two maximally separated nodes on an M by N resistor network. *Phys Rev E*, 82(1):011125. <https://doi.org/10.1103/PhysRevE.82.011125>
- Izmailian NS, Kenna R, 2015. The two-point resistance of fan networks. *Chin J Phys*, 53(1):126-136. <https://doi.org/10.6122/CJP.20141020A>
- Izmailian NS, Kenna R, 2014. A generalised formulation of the laplacian approach to resistor networks. *J Stat Mech: Theory Exp*, 9:P09016. <https://doi.org/10.1088/1742-5468/2014/09/P09016>
- Izmailian NS, Kenna R, Wu FY, 2014. The two-point resistance of a resistor network: a new formulation and application to the cobweb network. *J Phys A: Math Theor*, 47(3):035003. <https://doi.org/10.1088/1751-8113/47/3/035003>
- Ji YX, Ni LT, Zhao C, et al., 2023. Tripfield: A 3D potential field model and its applications to local path planning of autonomous vehicles. *IEEE Trans Intell Transp Syst*, 24(3):3541-3554. <https://doi.org/10.1109/TITS.2022.3231259>
- Jiang XY, Zhang GJ, Zheng YP, et al., 2024. Explicit potential function and fast algorithm for computing potentials in $\alpha \times \beta$ conic surface resistor network. *Expert Syst Appl*, 238:122157. <https://doi.org/10.1016/j.eswa.2023.122157>
- Jiang ZL, Wang WP, Zheng YP, et al., 2019. Interesting Explicit Expressions of Determinants and Inverse Matrices for Foeplitz and Loeplitz Matrices. *Mathematics*, 7(10):939. <https://doi.org/10.3390/math7100939>
- Jiang ZL, Zhou YF, Jiang XY, et al., 2023. Analytical potential formulae and fast algorithm for a horn torus resistor network. *Phys Rev E*, 107(4):044123. <https://doi.org/10.1103/PhysRevE.107.044123>
- Jin L, Qi YM, Luo X, et al., 2022a. Distributed competition of multi-robot coordination under variable and switching topologies. *IEEE Trans Automat Sci Eng*, 19(4):3575-3586. <https://doi.org/10.1109/TASE.2021.3126385>
- Jin L, Zheng X, Luo X, 2022b. Neural dynamics for distributed collaborative control of manipulators with time delays. *IEEE/CAA J Automat Sin*, 9(5):854-863. <https://doi.org/10.1109/JAS.2022.105446>
- Kirchhoff G, 1847. Ueber die auflösung der gleichungen, auf welche man bei der untersuchung der linearen vertheilung galvanischer ströme geführt wird. *Ann Phys*, 148(12):497-508. <https://doi.org/10.1002/andp.18471481202>
- Klein DJ, Randić M, 1993. Resistance distance. *J Math Chem*, 12(1):81-95. <https://doi.org/10.1007/BF01164627>
- Klein DJ, 2010. Centrality measure in graphs. *J Math Chem*, 47(4):1209-1223. <https://doi.org/10.1007/s10910-009-9635-0>
- Kook W, 2011. Combinatorial Green's function of a graph and applications to networks. *Adv Appl Math*, 46(1-4):417-423. <https://doi.org/10.1016/j.aam.2010.10.006>
- Kulathunga G, 2022. A reinforcement learning based path planning approach in 3D environment. *Procedia Comput Sci*, 212:152-160. <https://doi.org/10.1016/j.procs.2022.10.217>
- Liu YJ, Meirer F, Krest CM, et al., 2016. Relating structure and composition with accessibility of a single catalyst particle using correlative 3-dimensional microscopy. *Nat Commun*, 7(1):12634. <https://doi.org/10.1038/ncomms12634>
- Luo XL, Tan ZZ, 2023. Fractional circuit network theory with n-V-structure. *Phys Scr*, 98(4):045224. <https://doi.org/10.1088/1402-4896/acc491>
- Mahulea C, Kloetzer M, González R, 2020. Path Planning of Cooperative Mobile Robots Using Discrete Event Models. Wiley-IEEE Press. <https://doi.org/10.1002/9781119486305>
- Mason JC, Handscomb DC, 2002. Chebyshev Polynomials. Chapman and Hall/CRC, New York, p.360. <https://doi.org/10.1201/9781420036114>
- Mazaheri H, Goli S, Nourollah A, 2024. Path planning in three-dimensional space based on butterfly optimization algorithm. *Sci Rep*, 14(1):2332. <https://doi.org/10.1038/s41598-024-52750-9>
- Meng QY, Zheng YP, Jiang ZL. Determinants and inverses of weighted Loeplitz and weighted Foeplitz matrices and their applications in data encryption. *J Appl Math Comput*, 68(6):3999-4015.
- Meng QY, Jiang XY, Jiang ZL, 2021. Interesting determinants and inverses of skew loeplitz and foeplitz matrices. *J Appl Anal Comput*, 11(6):2947-2958. <https://doi.org/10.11948/20210070>
- Meng QY, Zheng YP, Jiang ZL, 2022. Exact determinants and inverses of (2,3,3)-Loeplitz and (2,3,3)-Foeplitz matrices. *Comp Appl math*, 41(1):35. <https://doi.org/10.1007/s40314-021-01738-6>
- Owaidat MQ, Hijjawi RS, Khalifeh JM, 2012. Network with two extra interstitial resistors. *Int J Theor Phys*, 51(10):3152-3159. <https://doi.org/10.1007/s10773-012-1196-5>
- Pan ZH, Zhang CX, Xia YQ, et al., 2022. An improved artificial potential field method for path planning and formation control of the multi-UAV systems. *IEEE Trans Circuits System II: Express Briefs*, 69(3):1129-1133. <https://doi.org/10.1109/TCSII.2021.3112787>

- Pennetta C, Alfinito E, Reggiani L, et al., 2004. Biased resistor network model for electromigration failure and related phenomena in metallic lines. *Phys Rev B*, 70(17):174305.
<https://doi.org/10.1103/PhysRevB.70.174305>
- Rhazaoui K, Cai Q, Adjiman CS, et al., 2013. Towards the 3D modeling of the effective conductivity of solid oxide fuel cell electrodes: I. model development. *Chem Eng Sci*, 99:161-170.
<https://doi.org/10.1016/j.ces.2013.05.030>
- Shi Y, Jin L, Li S, et al., 2022. Novel discrete-time recurrent neural networks handling discrete-form time-variant multi-augmented Sylvester matrix problems and manipulator application. *IEEE Trans Neural Netw Learn Syst*, 33(2):587-599.
<https://doi.org/10.1109/TNNLS.2020.3028136>
- Sun ZB, Wang G, Jin L, et al., 2022. Noise-suppressing zeroing neural network for online solving time-varying matrix square roots problems: A control-theoretic approach. *Expert Syst Appl*, 192:116272.
<https://doi.org/10.1016/j.eswa.2021.116272>
- Tan ZZ, Fang JH, 2015. Two-point resistance of a cobweb network with a $2r$ boundary. *Commun Theor Phys*, 63(1):36.
<https://doi.org/10.1088/0253-6102/63/1/07>
- Tan ZZ, Tan Z, 2020a. The basic principle of $m \times n$ resistor networks. *Commun Theor Phys*, 72(5):055001.
<https://doi.org/10.1088/1572-9494/ab7702>
- Tan ZZ, Tan Z, 2020b. Electrical properties of an $m \times n$ rectangular network. *Phys Scr*, 95(3):035226.
<https://doi.org/10.1088/1402-4896/ab5977>
- Tan ZZ, Tan Z, 2020c. Electrical properties of $m \times n$ cylindrical network. *Chin Phys B*, 29(8):080503.
<https://doi.org/10.1088/1674-1056/ab96a7>
- Tan ZZ, Zhou L, Yang JH, 2013. The equivalent resistance of a $3 \times n$ cobweb network and its conjecture of an $m \times n$ cobweb network. *J Phys A: Math Theor*, 46(19):195202.
<https://doi.org/10.1088/1751-8113/46/19/195202>
- Tan ZZ, 2017. Recursion-transform method and potential formulae of the $m \times n$ cobweb and fan networks. *Chin Phys B*, 26(9):090503.
<https://doi.org/10.1088/1674-1056/26/9/090503>
- Tan ZZ, 2022. Resistance theory for two classes of n-periodic networks. *Eur Phys J Plus*, 137(5):546.
<https://doi.org/10.1140/epjp/s13360-022-02750-3>
- Tan ZZ, 2023. Electrical property of an $m \times n$ apple surface network. *Results Phys*, 47:106361.
<https://doi.org/10.1016/j.rinp.2023.106361>
- Tan ZZ, 2023. Theory of an $m \times n$ apple surface network with special boundary. *Commun Theor Phys*, 75(6):065701.
<https://doi.org/10.1088/1572-9494/acb82>
- Tzeng WJ, Wu FY, 2006. Theory of impedance networks: the two-point impedance and LC resonances. *J Phys A: Math Gen*, 39(27):8579.
<https://doi.org/10.1088/0305-4470/39/27/002>
- Udrea G, 1996. A note on the sequence $(w_n)_{n \geq 0}$ of AF Horadam. *Port Math*, 53(2):143-156.
<http://eudml.org/doc/47619>
- Uğur A, 2008. Path planning on a cuboid using genetic algorithms. *Inform Sci*, 178(16):3275-3287.
<https://doi.org/10.1016/j.ins.2008.04.005>
- Wang JJ, Zheng YP, Jiang ZL, 2023. Norm equalities and inequalities for tridiagonal perturbed toeplitz operator matrices. *J Appl Anal Comput*, 13(2):671-683.
<https://doi.org/10.11948/20210489>
- Wang XZ, Che ML, Wei YM, 2017. Complex-valued neural networks for the Takagi vector of complex symmetric matrices. *Neurocomputing*, 223:77-85.
<https://doi.org/10.1016/j.neucom.2016.10.034>
- Wei YL, Jiang XY, Jiang ZL, et al., 2019a. Determinants and inverses of perturbed periodic tridiagonal Toeplitz matrices. *Adv Differ Equ*, 2019(1):410.
<https://doi.org/10.1186/s13662-019-2335-6>
- Wei YL, Zheng YP, Jiang ZL, et al., 2019b. A study of determinants and inverses for periodic tridiagonal Toeplitz matrices with perturbed corners involving Mersenne numbers. *Mathematics*, 7(10):893.
<https://doi.org/10.3390/math7100893>
- Wei YL, Jiang XY, Jiang ZL, et al., 2020. On inverses and eigenpairs of periodic tridiagonal toeplitz matrices with perturbed corners. *J Appl Anal Comput*, 10(1):178-191.
<https://doi.org/10.11948/20190105>
- Wei YL, Zheng YP, Jiang ZL, et al., 2022. The inverses and eigenpairs of tridiagonal Toeplitz matrices with perturbed rows. *J Appl Math Comput*, 68(1):623-636.
<https://doi.org/10.1007/s12190-021-01532-x>
- Wu FY, 2004. Theory of resistor networks: the two-point resistance. *J Phys A: Math Gen*, 37(26):6653-6673.
<https://doi.org/10.1088/0305-4470/37/26/004>
- Wu WQ, Zhang YN, 2024. Zeroing neural network with coefficient functions and adjustable parameters for solving time-variant sylvester equation. *IEEE Trans Neural Netw Learn Syst*, 35(5):6757-6766.
<https://doi.org/10.1109/TNNLS.2022.3212869>
- Xu GY, Eleftheriades GV, Hum SV, 2021. Analysis and design of general printed circuit board metagratings with an equivalent circuit model approach. *IEEE Trans Antennas Propagat*, 69(8):4657-4669.
<https://doi.org/10.1109/TAP.2021.3060084>
- Xue JM, Li J, Chen JY, et al., 2021. Wall-climbing Robot Path Planning for Cylindrical Storage Tank Inspection Based on Modified A-star Algorithm. *IEEE Far East NDT New Technology & Application Forum (FENDT)*, p.191-195.
<https://doi.org/10.1109/FENDT54151.2021.9749634>
- Yang YJ, Klein DJ, 2013. A recursion formula for resistance distances and its applications. *Discrete Appl Math*, 161(16-17):2702-2715.
<https://doi.org/10.1016/j.dam.2012.07.015>
- Yu ZH, Yuan J, Li YS, et al., 2023. A path planning algorithm for mobile robot based on water flow potential field method and beetle antennae search algorithm. *Comput Electr Eng*, 109:108730.
<https://doi.org/10.1016/j.compeleceng.2023.108730>
- Zhang D, Yang B, Tan JP, et al., 2021. Impact damage localization and mode identification of cfrps panels using an electric resistance change method. *Compos Struct*, 276:114587.
<https://doi.org/10.1016/j.compstruct.2021.114587>
- Zhao WJ, Zheng YP, Jiang XY, et al., 2023. Two optimized novel potential formulas and numerical algorithms for $m \times n$ cobweb and fan resistor networks. *Sci Rep*, 13(1):12417.
<https://doi.org/10.1038/s41598-023-39478-8>

- Zhou YF, Zheng YP, Jiang XY, et al., 2022. Fast algorithm and new potential formula represented by chebyshev polynomials for an $m \times n$ globe network. *Sci Rep*, 12(1):21260.
<https://doi.org/10.1038/s41598-022-25724-y>
- Zhou YF, Jiang XY, Zheng YP, et al., 2023. Exact novel formulas and fast algorithm of potential for a hammock resistor network. *AIP Adv*, 13(9):095127.
<https://doi.org/10.1063/5.0171330>
- Zhu ZX, Yin Y, Lü HG, 2023. Automatic collision avoidance algorithm based on route-plan-guided artificial potential field method. *Ocean Eng*, 271:113737.
<https://doi.org/10.1016/j.oceaneng.2023.113737>

unedit